

---

## ALKALI ACTIVATED CRAB SHELL FOR THE ADSORPTION OF VICTORIA BLUE FROM AQUEOUS SOLUTION

---

Hassan Ahmed El-Adawy<sup>1,2</sup>

<sup>1</sup>Chemistry Department, Faculty of Science, Al-Azhar University, Cairo, 11884, (EGYPT)

<sup>2</sup>Chemistry Department, Faculty of Science, Al-Baha University, EL-Mekhwa, 1988, (KSA)

---

### ABSTRACT

*In this study, the adsorption equilibrium of Victoria blue (VB) dye by alkali activated crab shell (AACS) was studied using batch process. The factors affecting the adsorption process, including contact time, pH, initial dye concentration, particle size, adsorbent dosage and temperature, were investigated. The models of Langmuir, Freundlich, and Temkin isotherms were used for analyze equilibrium data. The Langmuir isotherm model was found to fit the best, and the maximum adsorption capacity was 8.6 mg/g at 35°C. Thermodynamic parameters, such as  $\Delta H$ ,  $\Delta G$ , and  $\Delta S$  were calculated. Negative values of  $\Delta G$  indicated that the overall adsorption was spontaneous. The characterization of adsorbent surface by FTIR confirmed that the AACS can adsorb VB dye from its solutions. Experimental results showed that the adsorption capacity increased with temperature and the AACS was an effective adsorbent for removing VB dye.*

**Keywords:** Adsorption, Victoria blue, Crab shell, Isotherms, Thermodynamics

### 1. INTRODUCTION

Discharge of colored wastewater from various industries such as those of food, paper, carpet, rubber, plastics, cosmetics, textile, etc., into natural streams has caused major problems. Some examples of this problems include increasing the toxicity and COD (chemical oxygen demand) of the effluent, and reducing the light penetration, with an impact on photosynthetic phenomena. Also the presence of dyes may cause allergic dermatitis, skin irritation, mutation, cancer, etc. In addition, biodegradation of some of dyes produce aromatic amines, which are highly carcinogenic [1].

Victoria Blue (VB) is a class of cationic triarylmethane dye that is not biodegradable and widely used for dyeing silk, wool and cotton [2]. It is also used for staining in microscopic work [3]. This dye is known to cause strong toxicity and coloration in the waste water and can produce irritation to respiratory system and eyes [4]. It may even cause tumour growth in some species of fish [5]. Many techniques are used for dye removal, adsorption is an efficient option for removing dyes from water and wastewater [6]. Activated carbon is the most popular and widely used adsorbent for dye effluent. It is effective for

removing organic compounds because of its large surface area, high adsorption capacity, and microporous structure, but its use is usually limited due to its high cost and difficult to regenerate [7]. Using waste materials to treat dye effluent is the most popular option, because of their eco-friendly and economic traits, ready availability, and low cost [8].

Crab shell (CS), an undesirable by-product which is produced in millions of tons annually [9]. Currently large amounts of CS are discarded as waste in soil environment. Numerous chemicals and microorganisms from the decomposition of these residues could generate pollutants to soil and air environment [10, 11]. Therefore, many approaches are carried out to solve this problem by converting this solid waste into useful products instead of disposing them in landfill. Crab shell is mainly constituted of  $MgCO_3$ ,  $CaCO_3$ , chitin biopolymer along with a proportion of lipids and some proteins. The functional groups of CS are amine ( $-NH$ ) and hydroxyl ( $-OH$ ) forming negatively charged sites of adsorption that can be exchanged for cationic dye. Several reports used shell waste biosorbent to treat wastewater, such as biosorption of As by crab shell [12], Acid Blue 25 by shrimp shell [13], and  $Ag^+$  by crab shell [14].

The aim of this work is to exploit the ability of AACs as a bio-adsorbent material for removing VB dye from textile effluents.

## 2. MATERIALS AND METHODS

### 2.1. Adsorbent (AACs) Preparation

CS was collected from a local market (Al-Mekhwa, Al-Baha, Saudi Arabia kingdom), and then washed with distilled water to remove all soluble impurities. After that, the CS was dried in sun for a long period until completely dried. To obtain a uniform size product, the dried shells were ground through a mixer and sieved to 20 - 30 and 30 - 40 mesh sizes sieve. The sieved powder was treated with 1% NaOH for 24 h, then filtered and rinsed with distilled water. The treated material was dried again at 105°C for 2 h, sealed in plastic bags, and stored until use.

### 2.2. Characterization of adsorbent (CS)

The surface functional groups of the crab shell used in this study were analyzed by FTIR (Perkin Elmer, model two) where the obtained spectra were recorded in the range 4000-400 cm<sup>-1</sup>.

### 2.3. Preparation of Adsorbate (VB)

Victoria blue (C.I. 44045, molecular formula C<sub>33</sub>H<sub>32</sub>ClN<sub>3</sub>, molecular weight = 506.1 g/mole; Merck, Germany) was used as an adsorbate in this study (Figure 1). The stock solution was prepared by dissolving 500 mg of VB in one liter of distilled water and the working solutions (3, 6, 12, 24, and 50 mg/L) were obtained by diluting with distilled water.

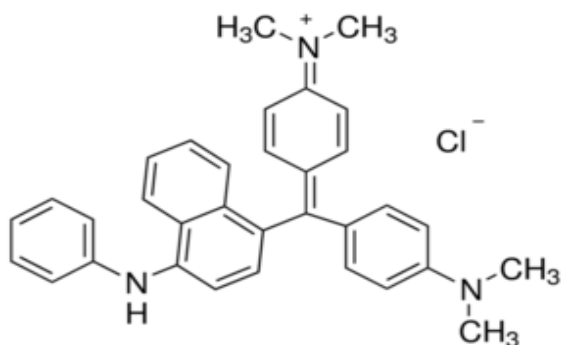


Figure 1. Molecular structure of Victoria blue

### 2.4. Procedures

Batch adsorption experiments were conducted by stirring a series of glass bottles containing 20 mL of VB solutions. The stirring proceeded with different adsorbent amounts of (0.5-3 g) and pH of 3 at room temperature for different time intervals (15-120 minutes) until the equilibrium reached, after which the adsorbent was filtered by filter paper. The absorbance of filtrate was determined by using UV-VIS spectrometer (UV-1800, SHIMADZU UV SPECTROPHOTOMETER) at adjusted  $\lambda_{\max} = 617$  nm. A suitable condition was set based on the previous procedures to carry out adsorption isotherms for VB dye onto AACs.

Three equilibrium isotherm models as Langmuir, Freundlich, and Temkin, were used to describe the experimental adsorption data. The Langmuir isotherm model is based on the assumption of monolayer coverage on a structurally homogeneous adsorbent, where all the adsorption sites are energetically equivalent and identical. The Langmuir isotherm in a linear form is represented as follows:

$$\frac{C_e}{q_e} = \frac{1}{q_m} C_e + \frac{1}{K_L q_m} \quad (1)$$

Where  $C_e$  (mg/L) is the equilibrium concentration,  $q_e$  (mg/g) is the amount adsorbed at equilibrium,  $K_L$  is the Langmuir constant, and  $q_m$  (mg/g) is the maximum adsorption capacity. The essential characteristics of a Langmuir isotherm can be expressed in terms of a dimensionless separation factor ( $R_L$ ), which is defined by:

$$R_L = \frac{1}{(1 + K_L C_o)} \quad (2)$$

where  $K_L$  is the Langmuir constant (dm<sup>3</sup> /mg) and  $C_o$  is the initial dye concentration (mol/dm<sup>3</sup>).

The Freundlich isotherm model is an empirical expression that encompasses the heterogeneity of the surface and the exponential distribution of sites and energies. The linear form of Freundlich isotherm is represented as follows:

$$\log q_e = \log K_f + \frac{1}{n} \log C_e \quad (3)$$

where  $K_f$  (L/g) is Freundlich constant and is called the adsorption capacity or the adsorption intensity. The Temkin isotherm assumes that the heat of adsorption of all molecules in a layer decreases linearly with the surface coverage of the adsorbent due to sorbate-adsorbate interactions. The Temkin isotherm in a linear form is represented as follows:

$$q_e = \frac{RT}{bT} \ln A + \frac{RT}{bT} \ln C_e \quad (4)$$

where  $RT/b_T$  is  $B$ ,  $A$ , Temkin isotherm constants (L/g) corresponding to the maximum binding energy,  $b_T$  is Temkin constant related to heat of sorption (J/mol),  $R$  is the gas constant (8.314 J/mol.K), and  $T$  is the absolute temperature (K).

### 3. Thermodynamics of adsorption

The thermodynamic parameters such as the Gibbs free energy ( $\Delta G^\circ$ ), the enthalpy ( $\Delta H^\circ$ ) and the entropy ( $\Delta S^\circ$ ) can be determined by using the following equations:

$$K_c = \frac{C_A}{C_S} \quad (5)$$

$$\Delta G^\circ = -RT \ln k_e \quad (6)$$

$$\ln K_c = -\frac{\Delta G^\circ}{RT} = \frac{\Delta H^\circ}{RT} + \frac{\Delta S^\circ}{R} \quad (7)$$

where  $K_c$  is the equilibrium constant,  $C_A$  and  $C_S$  are equilibrium concentrations (mg/g) of the dye in the solid and the liquid phases respectively,  $T$  is the absolute temperature in Kelvin and  $R$  is the gas constant. The linear plots of  $\ln K_c$  vs  $1/T$  yields  $\Delta H^\circ$  and  $\Delta S^\circ$  in the parameters form of slope and intercept respectively.

### 4. CALCULATIONS

The amount of dye adsorbed at equilibrium  $q_e$  (mg/g) was calculated using the following Equation:

$$q_e = \frac{(C_o - C_e)V}{m} \quad (8)$$

where  $C_o$  and  $C_e$  (mg/L) are the concentrations of dye solution at initial and equilibrium respectively,  $V$  (L) is the volume of the solution, and  $m$  (g) is the mass of the adsorbent used.

The amount of dye adsorbed at time  $t$ ,  $q_t$  (mg/g), was calculated using:

$$q_t = \frac{(C_e - C_t)V}{m} \quad (9)$$

The extent of adsorption is expressed in percentage as removal efficiency (%R) and is calculated using:

$$\% R = \frac{(C_o - C_t)V}{C_o} \quad (10)$$

## 5. RESULTS AND DISCUSSION

### 5.1. Characterization of crab shell before and after adsorption

To investigate the surface characteristics of AACS, FTIR spectra were performed in the range of 400 to 4000  $\text{cm}^{-1}$ . Figure 2(a) and Figure 2(b) represent the FTIR spectra of AACS before and after adsorption, respectively. In Figure 2(a), the wide, strong, and broad band at around 3269  $\text{cm}^{-1}$  is due to O-H and N-H stretching. The peak at 2919  $\text{cm}^{-1}$  is due to N-H and O-H stretching. The strong band observed at 1626  $\text{cm}^{-1}$  corresponds to N-H stretching. The peak around 1537  $\text{cm}^{-1}$  is due to N-H stretching of the amino groups. The band at 1027  $\text{cm}^{-1}$  is assigned to C-N bending. The strong band at 1397  $\text{cm}^{-1}$  is due to C=O stretching. The bands at 870  $\text{cm}^{-1}$  is due to the  $\beta$ -D-glucose unit of polysaccharide [15]. The peak positions of the major bands in the spectrum of CS saturated with VB (Figure 2(b)) are shifted from the same positions as in the spectrum of raw AACS. In addition, there are new and stronger peaks at 1152.7  $\text{cm}^{-1}$  due to C=O stretching, 1308  $\text{cm}^{-1}$  due to C-N vibration, and 1010  $\text{cm}^{-1}$  due to C-O stretching.

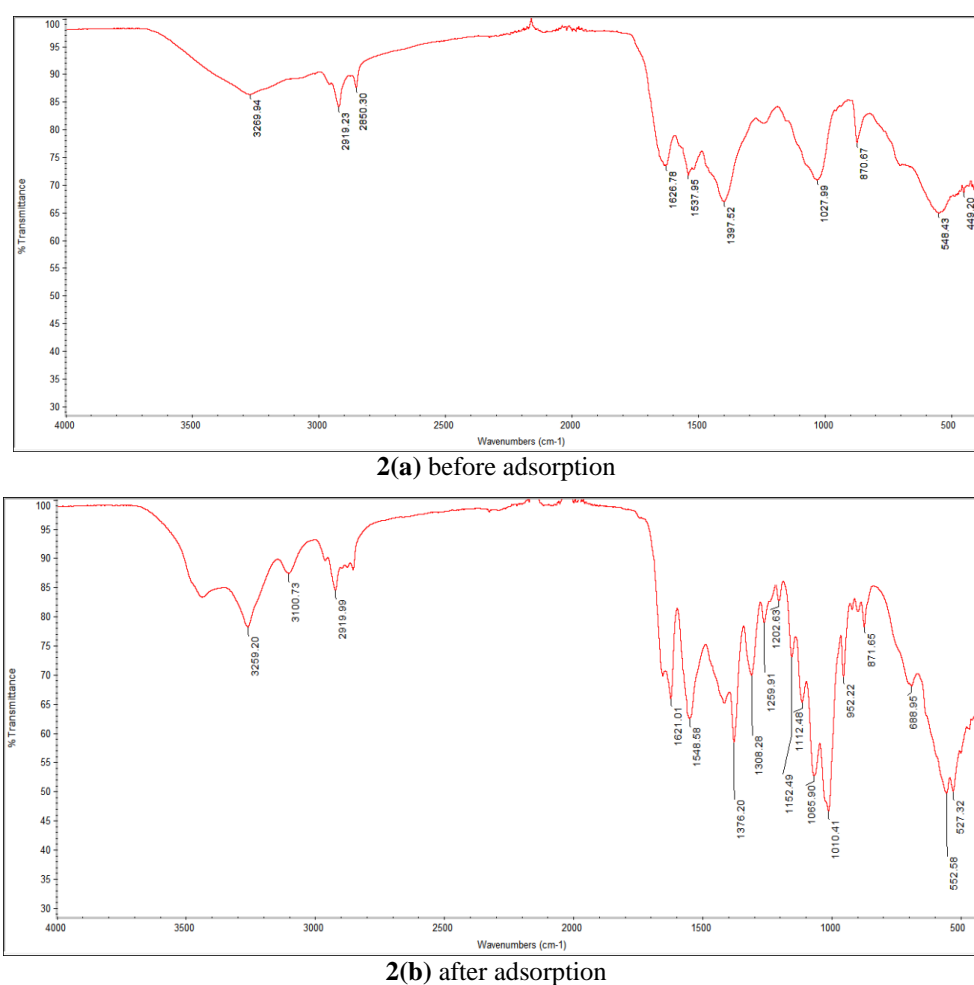


Figure 2. FTIR spectra of AACS before and after adsorption of VB.

## 5.2. Effect of pH

pH is an important factor in controlling the removal of VB dye onto AACS adsorbent. The removal of VB dye on AACS was studied at room temperature of  $298 \pm 4.0^\circ \text{K}$  and initial dye concentration of 24 mg/L by varying the pH from 2.0 to 12.0, the solution was equilibrated for 2 hours. The obtained results indicates that AACS adsorbent exhibit better removal capacity in alkaline medium than in acidic medium (Figure 3). The percentage removal of VB dye by adsorption on AACS increases by increasing the pH of the solution from 2.0 to 12.0. Low pH leads to an progressively increase in  $\text{H}^+$  ions concentration in the solution and the surface of the AACS acquires positive charge by absorbing  $\text{H}^+$  ions. As a result, significant repulsion occurs

between the positively charged CS surface and cationic dye molecules, leading to low adsorption. High pH leads to an increase in the negatively charged sites on CS which favor the adsorption of cationic dye molecules due to electrostatic attraction.

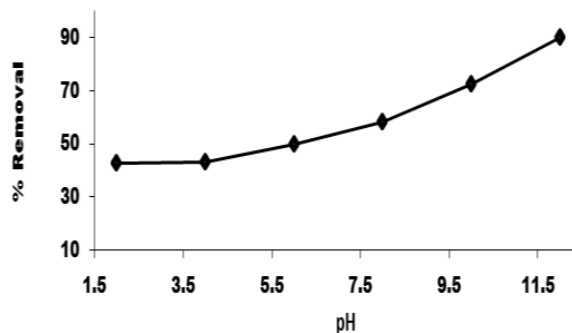
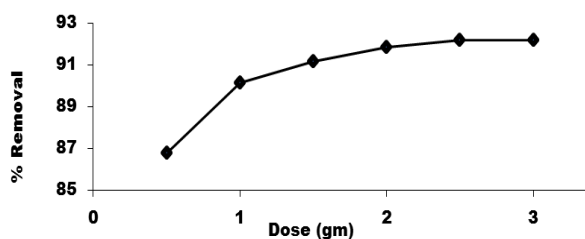


Figure 3. Effect of pH on VB removal using AACS

### 5.3. Effect of Adsorbent Dosage

The effect of adsorption dosage has been studied by varying adsorbent dosage over a range of 0.5 to 3.0 gm at a fixed initial VB dye concentration of 24 mg/L, pH of 12 and optimum contact time of 120 min and the obtained data are shown in figure 4. It can be observed that the percentage removal increased from 86.7% to 90.1% with the increase in adsorbent dose from 0.5 to 1.0 gm for AACs. The maximum percentage removal reached at a dosage of 2.5 gm per 1000 ml of VB dye solution, above which, the percentage removal smooth and slowly increased till saturation. This can be attributed to the increased adsorbent surface area and thus the availability of more adsorption sites with the increase of adsorbent dosage.



**Figure 4.** Effect of dosage on VB % removal (% R) using AACs

### 5.4. Effect of the particle size

Figure 5 depicts a plot of percent removal (%) versus time at different particle sizes. As the particle size decreased, the adsorption capacity of the AACs increased. As the particle size decreases from 20-30 mesh to 30-40 mesh, the adsorption capacity increased from 89 to 91%. An increase in capacity with decreasing particle size strongly suggests that dye does not completely penetrate the particle pores Walker [16] attributed this to the crushing process, the breaking up large particles resulting in the opening of tiny sealed channels in the adsorbent that then might become susceptible to adsorption. For larger particles, the diffusion resistance to mass transport is higher and it may be possible that most of the internal surface of the particle not be utilized for adsorption and consequently the amount of dye adsorbed is small. The surface

area of a non-porous adsorbent considerably increases with a decrease in particle size. Consequently, the adsorptive capacity should increase with a reduction in particle diameter.

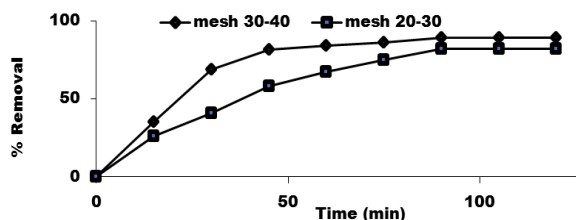


**Figure 5.** Effect of particle size on % removal (% R) of VB using AACs.

### 5.5. Effect of initial dye concentration

An increase of uptake is observed with increase in initial dye concentration due to an enhanced driving force for mass transfer. Experiments were conducted at different initial concentrations (3, 6, 12, 24 and 50 mg/L), and the observed uptake at different time intervals is shown in Figure 6. The rate of uptake was maximum in the beginning; then decreases with time, and ultimately stabilizes after  $t = 90$  min (all experiments were conducted for 120 min to ensure equilibrium). The concentration of both phases changes simultaneously with time; and hence, the concentration difference is the driving force for mass transfer. This is why uptake decreases with time and is constant at equilibrium. The best concentration used is 24 mg/L and after this, the uptake of VB dye on the AACs is minor so this concentration used in all experiments.

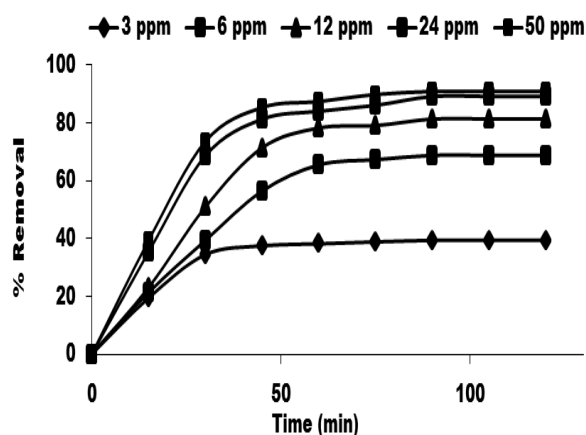


**Figure 6.** Effect of initial dye concentration on % removal (% R) of VB using AACs.

### 6.6. Effect of Temperature:

The effect of temperature on adsorption of dye solution with initial concentration of 24 mg/L and alkaline pH and at different temperatures: 308, 318, and 328°K has been determined. The results of the adsorption rates of VB dye at different temperatures are depicted in figure 7. The results indicate that the adsorption capacity of AACS for VB dye increased with temperature. This may be a result of increase in the mobility of the large dye ion with temperature. The increased number of molecules may also acquire sufficient energy to undergo an interaction with active sites at the surface. Moreover, increasing the temperature may produce a swelling effect within the internal structure of the adsorbent that enable large dyes to penetrate further.

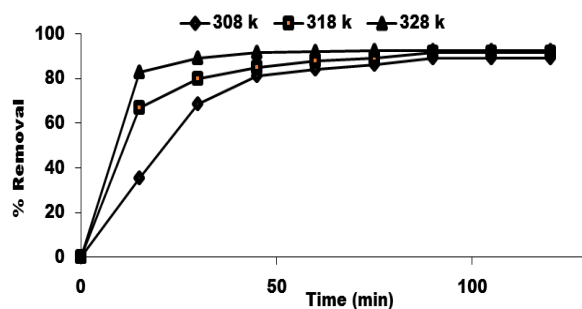


Figure 7. Effect of temperature on % removal (% R) of VB using AACS.

### 6.7. Langmuir adsorption isotherm

As shown in Fig.8, the plot of  $C_e/q_e$  versus  $C_e$  was linear (Figure 8), with a slope equal to  $1/q_{max}$  and an intercept equal to  $1/(q_{max} K_L)$ . The correlation coefficient,  $R^2$ , and the values of  $q_{max}$  and  $K_L$  for AACS sample studied are listed in table 1. The  $R^2$  value of 0.985 for AACS sample indicates that the adsorption of VB onto AACS sample is well fitted by the Langmuir isotherm. The value of  $R_L$  indicates whether the type of isotherm observed is unfavorable ( $R_L > 1$ ), linear ( $R_L = 1$ ) or favorable ( $R_L < 1$ ) [17]. The  $R_L$  values of adsorption of VB onto AACS are listed in table 3. along with the other Langmuir constants. The  $R_L$  values were in the range of  $0 < R_L < 1$  (0.88), indicating that the adsorption process was favorable.

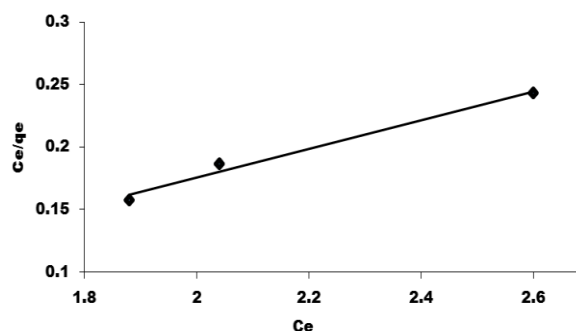


Figure 8. Langmuir adsorption isotherm of VB onto AACS surface

Table 1. Langmuir constants for the adsorption of VB onto the AACS.

adsorbent	Langmuir isotherm constants			
	$q_{max}$ (mg g <sup>-1</sup> )	$K_L$ (dm <sup>3</sup> /mg)	$R_L$	$R^2$
AACS	8.6	18.24	0.88	0.985

### 6.8. Freundlich adsorption isotherm

The plot of  $\log q_e$  versus  $\log C_e$  was linear as seen in figure 9, with a slope equal to  $1/n$  and an intercept equal to  $\log K_f$ . The correlation coefficient,  $R^2$  is also showed in table 2. The constant  $K_f$  is an approximate indicator of adsorption capacity, while  $1/n$  is a function of the strength of adsorption in the adsorption process. If a value of  $1/n$  is below one it indicates a normal adsorption. On the other hand,  $1/n$  being above one indicates cooperative adsorption. This expression reduces to a linear adsorption isotherm when  $1/n = 1.0$ . If  $n$  lies between 1.0 to 10, this indicates a favorable adsorption process [18]. From the parameters summarized in table 2, a value of  $1/n = 0.2$  while  $n = 4.9$  confirms that the adsorption of VB onto the AACS is favorable.

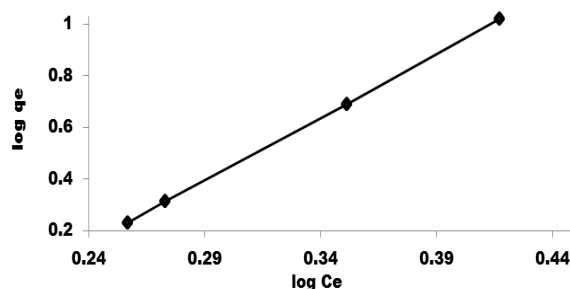


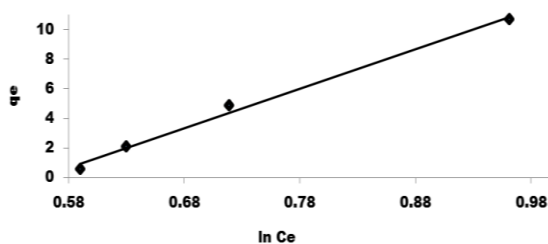
Figure 9. Freundlich adsorption isotherm of VB onto AACS surface

**Table 2.** Freundlich constants for the adsorption of VB onto the AACS sample.

adsorbent	Freundlich isotherm constants			
	1/n	n	K <sub>f</sub> (mg <sup>-1</sup> )	R <sup>2</sup>
AACS	0.2	4.9	1.03	0.99

### 6.9. Temkin Isotherm

From the Temkin plot ( $q_e$  versus  $\ln C_e$ ); A (slope) = Temkin isotherm equilibrium binding constant (L/g); b (intercept) = Temkin isotherm constant; while R = universal gas constant (8.314 J·mol<sup>-1</sup>·K<sup>-1</sup>) T= Temperature at 308° K, as shown in figure 10 and listed in table 3. The heat of VB adsorption (b) is directly related to coverage of VB onto AACS due to adsorbent-adsorbate interaction. Analysis of Temkin constants for VB dye removal showed high value of both adsorption capacity, A, (1.5 L/g) and high value of R<sup>2</sup> (0.99). Thus, although the data is better fitted by Langmuir, it can also be modeled by the Temkin isotherm, as supported by the greater coefficient of correlation (R<sup>2</sup>). Furthermore, the constant b<sub>T</sub> reflecting the bonding energy which in turn dictates the type of interaction, was of low value (0.095 kJ/mol) which reveals that the interactions between the VB dye and AACS are neither proceeding purely through ion-exchange nor taking place purely through physisorption.

**Figure 10.** Temkin adsorption isotherm of VB onto AACS surface**Table 3.** Temkin constants for the adsorption of VB onto the crab shell sample.

adsorbent	Temkin isotherm constants			
	B=RT/br	b <sub>T</sub> (kJ/mol)	A (L/g)	R <sup>2</sup>
AACS	26.71	0.095	1.5	0.99

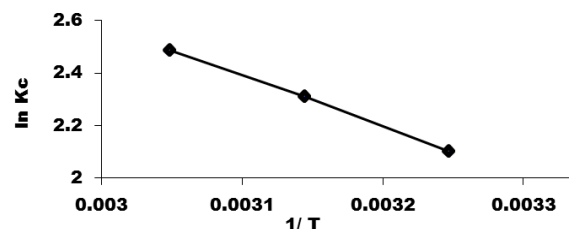
### 6.10. Thermodynamic studies

As derived from the plots of the experimental data obtained at different

temperatures, the calculated thermodynamic parameters for the adsorption of VB onto AACS are given in table 4.  $\Delta G^\circ$  values are obtained from equation (12),  $\Delta H^\circ$  and  $\Delta S^\circ$  values are obtained from the slope and intercept of plot  $\ln K_c$  against  $1/T$ , as represented in figure 11 and summarized in table 4. The adsorption is endothermic due to the positive values of  $\Delta H^\circ$ , while positive values of  $\Delta S^\circ$  indicate increased randomness at liquid-solid interface and therefore increase in adsorbate concentration on solid phase during sorption process. All the values of  $\Delta G^\circ$  are negative values indicate feasibility and spontaneity of the process.

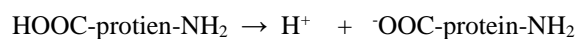
**Table 4.** Thermodynamic parameters for the adsorption of VB onto AACS.

Temperature (K)	Temkin isotherm constants		
	$\Delta G^\circ$ (kJ/mol)	$\Delta H^\circ$ (kJ/mol)	$\Delta S^\circ$ (kJ/mol)
308	- 0.61	16.15	0.06
318	- 0.69		
328	- 0.72		

**Figure 11.** Von't Hoff plot for effect of temperature on adsorption of VB onto AACS

### 6.11. The adsorption mechanism

The mechanism of adsorptive removal of VB dye by AACS sample is shown in the following scheme. The AACS contains high percent of proteins which are ionized to negative sites of carboxylic groups. On the other hand the basic dye VB is ionized to cationic and colorless anions, so, one can concluded that, there is an electrostatic interaction between the cations of VB dye and the negative sites of protein.



## 7. CONCLUSIONS

Alkali activated crab shell (AACS) has negatively charged surface and imparts electrostatic attraction towards cationic dye. Maximum 91% of Victoria Blue dye was removed. For the present AACS sample, which was collected from Al-Mekhwa, Al-Baha, KSA, a negatively charged protein imparted electrostatic attraction towards cationic dye. The adsorption data for VB investigated in this work fitted well to Langmuir, Freundlich, and Tekmin adsorption isotherms equations. The present study indicates that natural AACS sample is a promising low cost adsorbent for the removal of VB dye from aqueous solution. Interestingly that colored dye adsorbed CS can be recovered for further use as a colorant in various application.

## REFERANCES

- [1] Azza, K., Ahmed, N., Amany, S., Ola, A., Removal of Direct N Blue-106 from artificial textile dye effluent using activated carbon from orange peel: Adsorption isotherm and kinetic studies, *Journal of Hazardous Materials*, 2009, 165, 100–110.
- [2] Schulte, E. and Wittekind, D., *Histochemistry*, 1988, 88, 427-433.
- [3] Cho, B. P., Yang, T., Blankenship, L. R., Moody, J. D., Churchwell, M., Beland, F. A. and Culp, S., *J. Chem. Res. Toxicol.*, 2003, 3, 285-294.
- [4] Delory, G. E. And King, E. J., *Biochem J.*, 1945, 39, 245.
- [5] Canan, V., Vlasoula, B., Mahmut, K., Numan, B., Ilker, O., Panagiotis, L., Gerasimos, L. and Siddik, I., *Journal of Hazardous Materials*, 2009, 170, 27-34.
- [6] Daneshvar, E., M.S. Sohrabi, M. Kousha, A. Bhatnagar, B. Aliakbarian, A. Converti, and A-C. Norrström. 2014. Shrimp shell as an efficient bioadsorbent for Acid Blue 25 dye removal from aqueous solution. *Journal of the Taiwan Institute of Chemical Engineers*. 45(6): 2926-2934. doi: 10.1016/j.jtice.2014.09.019
- [7] Low, L.W., T.T. Teng, F. M. Alkarkhi, Abbas, A. Ahmad, and N. Morad. 2011. Optimization of the Adsorption Conditions for the Decolorization and COD Reduction of Methylene Blue Aqueous Solution using Low-Cost Adsorbent. *Water Air Soil Pollute*. 214, 185-195. doi: 10.1007/s11270-010-0414-0
- [8] Chowdhury, S., R. Mishra, P. Saha, and P. Kushwaha. Adsorption thermodynamics, kinetics and isosteric heat of adsorption of malachite green onto chemically modified rice husk. *Desalination*, 2011, 265, 159-168. doi: 10.1016/j.desal.2010.07.047
- [9] Lu S, Gibb SW, Cochrane E. Effective removal of zinc ions from aqueous solution using crab Carapace biosorbent. *J Hazard Mater* 2007, 149, 208–217.
- [10] Ramdani N, Wang J, He X-y, Feng T-t, Xu X-d, Liu W-b, etal. Effect of crab shell particles on the thermomechanical and thermal properties of polybenzoxazine matrix. *Mater Des*, 2014, 61, 1–7.
- [11] Vijayaraghavan K, Winnie HYN, alasubramanian R. Biosorption characteristics of crab shell particles for the removal of manganese (II) and zinc (II) from aqueous solutions. *Desalination*, 2011; 266, 195–200.
- [12] Rahman, M. A., M. M. Hossain, A. Samad, and A. M. Shafiqul Alam. Removal of Arsenic from Ground Water with Shrimp Shell. *Dhaka University Journal of Science*, 2012, 60(2), 175-180.
- [13] Daneshvar, E., M.S. Sohrabi, M. Kousha, A. Bhatnagar, B. Aliakbarian, A. Converti, and A-C. Norrström. 2014. Shrimp shell as an efficient bioadsorbent for Acid Blue 25 dye removal from aqueous solution. *Journal of the Taiwan Institute of Chemical Engineers*. 2014, 45(6), 2926-2934. doi: 10.1016/j.jtice.2014.09.019
- [14] Joen, C. Adsorption characteristics of waste crab shells for silverions in industrial wastewater. *Korean Journal of Chemical Engineering*, 2014, 31(3), 446-451. doi: 10.1007/s11814-013-0234-1
- [15] Kamala, K., P. Sivaperumal, and R. Rajaram. Extraction and Characterization of Water Soluble Chitosan from *Parapeneopsis Stylifera* Shrimp Shell Waste and Its Antibacterial Activity. *International Journal of Scientific and Research Publications*. 2013, 3(4), 1-8.
- [16] G. Walker. Industrial wastewater treatment using biological activated carbon, PhD Thesis, Queen's University Belfast, Belfast, UK, 1995.
- [17] Koswojo, R., Utomo, R. P., Y.-H. Ju, Ayucitra, A., Soetaredjo, F. E., Sunarso, J. and Ismadji, S., *Applied Clay Science*, 2010, 48, 81-86.
- [18] Goldberg, S., *Soil Science Society of America, Chemical Processes in Soils. SSSA Book Series*, no. 8.2005.